

SplitNet: Sim2Sim and Task2Task Transfer for Embodied Visual Navigation

Daniel Gordon^{1*} Abhishek Kadian² Devi Parikh^{2,3} Judy Hoffman^{2,3} Dhruv Batra^{2,3}

¹Paul G. Allen School of Computer Science, University of Washington

²Facebook AI Research ³Georgia Institute of Technology

Abstract

We propose *SplitNet*, a method for decoupling visual perception and policy learning. By incorporating auxiliary tasks and selective learning of portions of the model, we explicitly decompose the learning objectives for visual navigation into perceiving the world and acting on that perception. We show dramatic improvements over baseline models on transferring *between simulators*, an encouraging step towards *Sim2Real*. Additionally, *SplitNet* generalizes better to unseen environments from the same simulator and transfers faster and more effectively to novel embodied navigation tasks. Further, given only a small sample from a target domain, *SplitNet* can match the performance of traditional end-to-end pipelines which receive the entire dataset^{1,2}.

1. Introduction

A longstanding goal of computer vision is to enable robots to understand their surroundings, navigate efficiently and safely, and perform a large variety of tasks in complex environments. A practical application of the recent successes in Deep Reinforcement Learning is to train robots with minimal supervision to perform these tasks. Yet poorly-trained agents can easily injure themselves, the environment, or others. These concerns, as well as the difficulty in parallelizing and reproducing experiments at a low cost, have drawn research interest towards simulation environments [3, 15, 35, 36, 20].

However no simulator perfectly replicates reality, and agents trained in simulation often fail to generalize to the real-world. Transferring learned policies from simulation to the real-world (Sim2Real) has become an area of broad interest [25, 27, 33] yet there still exists a sizable performance gap for most algorithms. Furthermore, Sim2Real transfer reintroduces safety and reproducibility concerns. To mitigate this, we explore the related task of Sim2Sim, transfer-

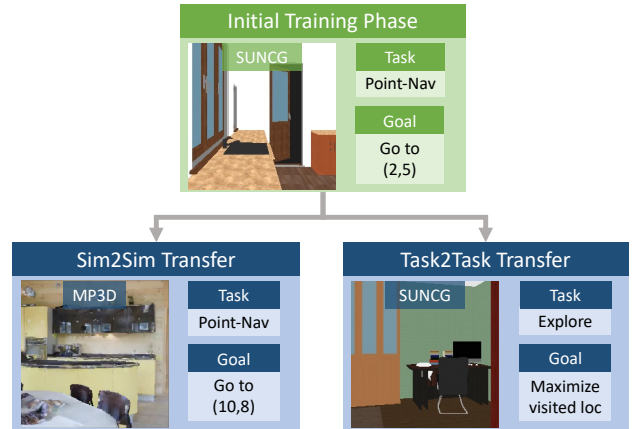


Figure 1. We decompose learning of visual navigation tasks into learning of a visual encoder and learning of an embodied task decoder. Through this decomposition we enable fast transfer to new visual environments and transfer to new embodied tasks.

ring policies between simulators, for embodied visual navigation (Figure 1). Transferring between simulators incurs a similar “reality gap” as between simulation and reality, due to differences in data collection and rendering. Learning to transfer between simulation environments serves as an encouraging preliminary step towards true Sim2Real transfer.

To enable Sim2Sim transfer we propose SplitNet, a composable model for embodied visual tasks which allows for the sharing and reuse of information between different visual environments. SplitNet enables transfer across different embodied tasks (Task2Task), meaning our model can learn new skills quickly and adapt to the ever-changing requirements of end users. Our key insight is to observe that embodied visual tasks are naturally decomposable into visual representation learning to extract task agnostic salient information from the visual input, and policy learning to interpret the visual representation and determine a proper action for the agent. Rather than learning these components solely independently or completely tied, we introduce an algorithm for learning these embodied visual tasks which benefits both from the scalability and strong in-domain, on-task performance of an end-to-end system and from the gen-

*Work done during an internship at Facebook AI Research.

¹<https://github.com/facebookresearch/splitnet>

²<https://youtu.be/TJkZcsD2vrc>

eralization and fast adaptability of modular systems.

SplitNet incorporates auxiliary visual tasks, such as depth prediction, as a source of intermediate supervision which guides the visual representation learning to extract information from the images extending beyond the initial embodied task. We demonstrate that initial pre-training of the visual representation on such auxiliary visual tasks produces a more robust initialization than the standard approach of pre-training on auxiliary visual datasets (e.g. ImageNet [5]) which may not be from an embodied perspective. Then we showcase the composability of our model by illustrating its ability to selectively adapt only the visual representation (when moving to a new visual environment) or only its policy (when moving to a new embodied task).

We center our evaluation on adapting between different simulators of varying fidelity and between different embodied tasks. Specifically, our experiments show that compared to end-to-end methods, SplitNet learns more transferable visual features for the task of visual point-to-point navigation, reduces overfitting to small samples from a new target simulator, and adapts faster and better to novel embodied tasks.

2. Related Work

This work introduces a learning approach for transferring visual representations between environments and for transferring policy information between different embodied tasks. The most related lines of work focus on adaptation and transfer of visual representations, deep reinforcement learning (especially from visual inputs), and transferring from simulation to the real-world (Sim2Real) both for visual and embodied tasks.

Visual Transfer and Adaptation. Many works have explicitly studied techniques for increasing the reusability of learned information across different visual tasks. Domain adaptation research has mainly focused on reusing a representation even as the input distribution changes, with most work focusing on representation alignment through explicit statistics [19, 31] or through implicit discrepancy minimization with a domain adversarial loss [6, 34]. A related line of work focuses on sharing between two image collections through direct image-to-image transfer [26, 40], whereby a mapping function is learned to take an image from one domain and translate it to mimic an image from the second domain [2, 10, 18, 32].

In parallel, many works focus on reusing learned representations for solving related visual tasks. The most prevalent such technique is simply using the first representation parameters as initialization for learning the second, termed finetuning [7]. A recent study proposed a technique for computing the similarity between a suite of visual tasks to create a Taskonomy [37] which may be used to determine, given a new task, which prior tasks should be used for

the initialization before continued learning. This method focuses on “passive” visual understanding tasks such as recognition, reconstruction and depth estimation and does not delve into learning representations for “active” tasks such as embodied navigation where an agent must both understand the world and directly use its understanding for some underlying task.

Overall, much of the prior work has focused on representation learning for visual recognition. In contrast, this work studies transfer of visuomotor policies for embodied tasks and decomposes the problem into transfer of visual representations for embodied imagery (Sim2Sim) and transfer of policies across various downstream embodied tasks (Task2Task).

Visual RL Tasks: In parallel with the development of deep representation learning for passive visual tasks, there has also been a plethora of recent research on policy learning from visual inputs inspired by the success of end-to-end visuomotor policy learning [16, 17, 22]. Much of the success here comes from training on large-scale [17] data, frequently made possible by extensive use of simulation environments [9, 22, 24, 42]. These techniques often leverage the additional supervision and auxiliary tasks given by the simulators to bootstrap their learning [21, 28]. Perceptual Actor [28] specifically examines how 20 different pre-training tasks affect the learning speed and accuracy of a visual navigation policy as compared to random initialization. Others use unsupervised [14] or self-supervised [24] learning as an additional signal in domains with sparse rewards. We build on these approaches by explicitly separating the auxiliary learning from the policy layers to ensure a decoupling of the weights which enables better transfer to new environments.

For increased task generalization, others have proposed using the successor representation [38, 41] which decomposes the reward and Q-functions into a state-action feature $\phi_{s,a}$, a successor feature $\psi_{s,a}$ and a task reward vector w . This decomposes the network into one which learns the dynamics of the environment separate from the specified task, which allows for faster transfer to new tasks by only retraining the task embedding w . Our proposed method allows quick transfer to new tasks as well as new environments.

Sim2Real: Significant progress has been made on adapting between simulated and real imagery for visual recognition, especially in the context of semantic segmentation in driving scenes [10, 11, 12, 39]. These techniques build on the visual domain adaptation methods described above. In parallel, there has been work on transferring visual policies learned in simulation to the real-world, but often limited to simple visual domains [27, 33] which bear little resemblance to the complexity of true real-world scenes. Rusu et al. [27] train a network in simulation before initializing

a new network which receives outputs from the simulation-trained network as well as real-world inputs. Yet their evaluation is limited to simple block picking experiments with no complex visual scenes. Peng et al. [25] use randomization over the robot dynamics to learn robust policies, but do not use visual inputs in simulation or reality and only perform simple puck-pushing tasks. Tobin et al. [33] randomize colors, lighting, and camera pose as a form of augmentation of the simulated imagery to better generalize to real-world imagery, but focus on primitive geometric objects for picking tasks.

A recent method [23], uses semantic segmentation as an intermediate objective to aid in transferring learned driving policies from simulation to the real-world. While we do not transfer our policies to real robots, we focus on visually diverse scenes which better match the complexity of the real-world than the simplistic setups of many of the prior policy transfer approaches. Similar to Müller et al. [23] we use auxiliary intermediate objectives to aid in transfer, but in our case focus on a set of auxiliary visual and motion tasks which generalize to many downstream embodied tasks and propose techniques to selectively transfer either across visual environments or across embodied tasks.

3. SplitNet: Decoupled Perception and Policy

Solving complex visual planning problems frequently requires different types of abstract understanding and reasoning based on the visual inputs. In order to learn compact representations and generalizable policies, it is often necessary to go beyond the end-to-end training paradigm. This is especially true when the initial learning setting (source domain) and current learning setting (target domain) have sufficiently different visual properties (e.g. differing visual fidelity as seen in Figure 1 left) or different objectives (e.g. transfer from one task to another as in Figure 1 right). In this section we outline the learning tasks we use, and our strategy for training a network which transfers to new visual domains and new embodied tasks.

3.1. Embodied Tasks

In this work, we focus on the following three visual navigation tasks which require memory, planning, and geometric understanding: Point-to-Point Navigation (Point-Nav), Scene Exploration (Exploration), and Run Away from Location (Flee). In our experiments, all tasks share a discrete action space: Move Forward by 0.25 meters and Rotate Left/Right by 10 degrees.

Point-to-Point Navigation (Point-Nav) An agent is directed to go to a point via a constantly updating tuple of (angle to goal, distance to goal). The agent succeeds if it ends the episode within a fixed radius of the goal. In our experiments we use a success radius of 0.2 meters and the agent is spawned anywhere from 1 to 30 meters from the

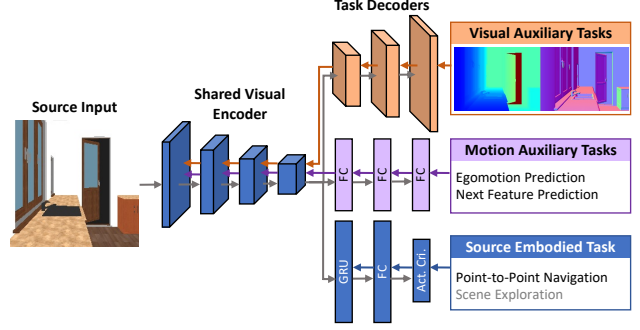


Figure 2. **SplitNet initial learning on source data and task.** Given source visual inputs, the visual encoder is trained using auxiliary visual and motion based tasks. Next, the policy decoder is trained on the source embodied tasks with a fixed visual encoder. Gradients from the embodied task (depicted as blue arrows) are stopped before the shared visual encoder to ensure decoupling of the policy and perception.

goal. The agent is provided with a one-hot encoding of its previous action. Since the agent is given the distance to the goal, learning the Stop action is trivial, so we disregard it.

Scene Exploration (Exploration) We discretize the world-space into 1 meter cubes and count the number of distinct cubes visited by the agent during a fixed duration. This task differs from Point-to-Point Navigation in that no absolute or relative spatial locations are provided to the agent. This prohibits agents from learning to detect collisions by comparing location values from two timesteps, requiring them to visually detect collisions. The agent still receives a one-hot encoding of its previous action.

Run Away from Location (Flee) The goal of this task is to maximize the geodesic distance from the start location and the agent’s final location in episodes of fixed length. As in Exploration, no spatial locations are given to the agent.

3.2. Decomposing the Learning Problem

For visual navigation tasks, an agent must **understand what it sees** and it must use the perceived world to **decide what to do**. Thus, we decompose visual navigation into the subtasks of (1) encoding the visual information and (2) using the encoded information to navigate. At each time t the agent receives an egocentric image I_t from the environment and must return a navigation action a_t in order to accomplish the task. Instead of learning actions directly from pixels, we break the decision-making into two stages. First, a function \mathcal{F} processes the image I_t producing a feature embedding $\phi_t = \mathcal{F}(I_t)$. Next, the features are decoded into an action $a_t = \mathcal{G}(\phi_t)$. Our goal is to learn features ϕ_t which extract salient information for completing navigation tasks and which generalize to new environments. Rather than passively expecting the end-to-end training to result in transferable features, we directly optimize portions of the

network with distinct objectives to produce representations which are highly semantically meaningful and transferable.

3.3. Visual Encoder

Visual understanding comes in many forms and is highly dependent on the desired end task. In the case of visual navigation, the agent must convert pixel inputs into an implicit or explicit geometric understanding of the environment’s layout. To encapsulate these ideas, we train a bottleneck encoder-decoder network supervised by several auxiliary visual and motion tasks. Each task uses a shared encoder, and produces a general purpose feature, ϕ_t . This feature is then used as input to learn a set of task specific decoders.

Auxiliary Visual Tasks: We encourage the shared encoder to extract geometric information from the raw visual input by augmenting the learning objective with the following auxiliary visual tasks: (1) prediction of depth through a depth decoder, \mathcal{D} , (2) prediction of surface normals through a surface normal decoder, \mathcal{S} , and (3) RGB reconstruction through a reconstruction decoder, \mathcal{R} (sample outputs are shown in the supplementary material). For an input image I_t with ground truth depth, D_t and ground truth surface normals S_t , the learning objective for each of these auxiliary visual decoders is as follows:

$$\mathcal{L}_D = \sum_{pixels} \|\mathcal{D}(\phi_t) - D_t\|_1 \quad (1)$$

$$\mathcal{L}_S = 1 - \sum_{pixels} \frac{\mathcal{S}(\phi_t) \cdot S_t}{\|\mathcal{S}(\phi_t)\|_2 * \|S_t\|_2} \quad (2)$$

$$\mathcal{L}_R = \sum_{pixels} \|\mathcal{R}(\phi_t) - I_t\|_1 \quad (3)$$

We use the ℓ_1 loss for reconstruction and depth to encourage edge sharpness. We use the cosine loss for the surface normals as it is a more natural fit for an angular output.

Auxiliary Motion Tasks: We additionally encourage the visual encoder to extract information which may be generically useful for future embodied tasks by adding the following auxiliary motion tasks: (1) predict the egomotion (discrete action) of the agent with motion decoder \mathcal{E} , and (2) forecast the next features given the current features and a one-hot encoding of the action performed with motion decoder \mathcal{P} . For a visual encoding ϕ_t at time t , previous encoding ϕ_{t-1} , and action a_t that causes the agent to move from I_{t-1} to I_t , the learning objective for each of these auxiliary motion decoders is as follows:

$$\mathcal{L}_E = - \sum_{a \in A} p(a_t = a) \log(\mathcal{E}(\phi_t, \phi_{t-1})) \quad (4)$$

$$\mathcal{L}_P = 1 - \sum_{features} \frac{\mathcal{P}(\phi_{t-1}, a_t) \cdot \phi_t}{\|\mathcal{P}(\phi_{t-1}, a_t)\|_2 * \|\phi_t\|_2} \quad (5)$$

We use the cross-entropy loss as we use a discrete action space, and we use the cosine loss for next feature prediction as it directly normalizes for scale which stops the network from forcing all the features arbitrarily close to 0.

All objectives affecting the learning of the visual encoder can be summarized in the joint loss:

$$\mathcal{L} = \lambda_R \mathcal{L}_R + \lambda_D \mathcal{L}_D + \lambda_S \mathcal{L}_S + \lambda_E \mathcal{L}_E + \lambda_P \mathcal{L}_P$$

where $\lambda_R, \lambda_D, \lambda_S, \lambda_E, \lambda_P$ are scalar hyperparameters which control the trade-off between the various tasks in this multi-task learning objective.

Rather than expecting our network to learn to extract geometric information decoupled from the policy decoders, we force the visual representation to contain this information directly. This decreases the likelihood of overfitting to training environments and thus increases the likelihood that our model generalizes to unseen environments.

3.4. Policy Decoder

Our policy decoder takes as input the visual features ϕ_t and learns to predict a desired action, a_{t+1} , supervised by a reward signal provided by the desired task. To avoid purely reactive policies, we employ a GRU [4] to add temporal context. The output of the policy layers predicts a probability distribution over the discretized action space and a value estimate for the current state. The probability distribution is sampled to determine which action to perform next.

When training the policy decoder, we fix our visual encoder and optimize only the policy decoder weights for the chosen task i.e. **gradients do not propagate from the source task to the visual layers** (see Figure 2 for an illustration of the gradient flow from the embodied task loss). This prevents policy information from leaking into the visual representation, ensuring the visual encoder generalizes well for many tasks. For the task of Point-to-Point Navigation we use two training strategies: **BC** and **BC, PPO**.

BC: We train the agent using behavioral cloning (BC) where the ground truth represents the action which would maximally decrease the geodesic distance between the current position and the goal. This is trained in a “student-forcing” regime i.e. the agent executes actions based on its policy, but evaluates the actions using the ground truth.

BC, PPO: We initialize the agent with the weights from the BC setting and update only the policy layers using the PPO algorithm [29] with a shaped reward based on the geodesic distance to the goal, $Geo(P, G)$:

$$r_t^{pointnav} = Geo(P_{t-1}, G) - Geo(P_t, G) + \lambda_T \quad (6)$$

where P_t is the agent’s location at time t , G is the goal location, and λ_T is a small constant time penalty.

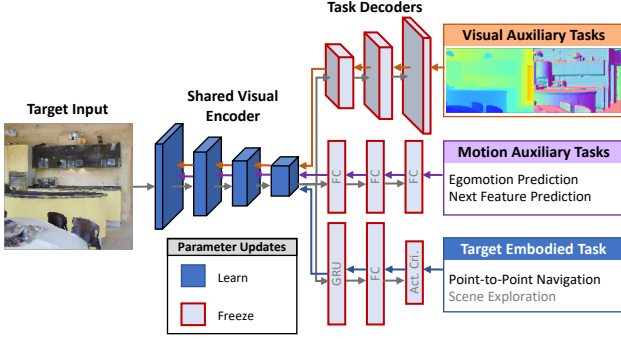


Figure 3. **SplitNet visual domain transfer.** When the target visual inputs differ from the source visual inputs while the desired embodied task remains fixed, our model updates the shared visual encoder using only auxiliary visual and motion based learning tasks. All decoder weights are frozen (to prevent overfitting), but gradients propagate through all decoder layers to the encoder.

3.5. Selective Transfer to New Domains and Tasks

3.5.1 Adapting to new Visual Domains

By decomposing the learning task into a perceptual encoder and a policy decoder, each supervised by their own objectives, our model is able to learn more transferable visual features than end-to-end methods. Furthermore, our model can quickly adapt its perceptual understanding with auxiliary visual and motion based training in the target environment without needing to modify the policy. Figure 3 illustrates the visual encoder adaptation learning procedure. Given a small sample of data and tasks in the target domain, we backpropagate gradients through the policy decoder³ and the auxiliary task layers **but freeze the weights for all but the shared visual encoder**. By doing so, our model can quickly adapt its perception without overfitting the policy to the small sample.

3.5.2 Adapting to new Tasks

When transferring to a new embodied task operating in the same visual space, our model only needs to update the policy decoder parameters (see Figure 4). While reusing lower-level features for new tasks by replacing and retraining the final layers is a common technique in deep learning [7, 13, 8] our model naturally decouples perception and reasoning offering a clear solution as to which layers to freeze or finetune. Rich perceptual features often transfer to tasks which require different reasoning assuming that the representation encodes the necessary information for the new task. By using auxiliary tasks to inform the updates to the visual encoder, we aim to encourage learning of intermediate features that capture semantically meaningful in-

³Without propagating gradients through the policy decoder, the encoder feature representation shifts and no longer matches the policy decoder.

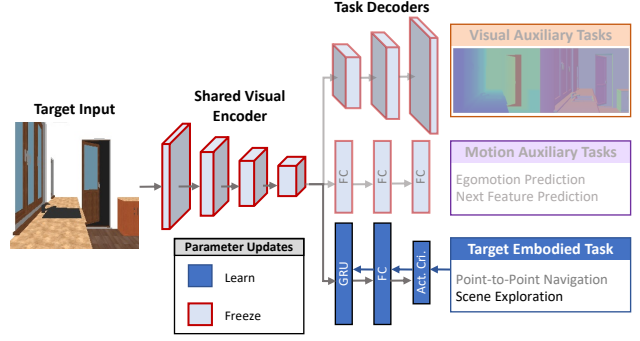


Figure 4. **SplitNet task transfer.** When learning a new embodied task for the same visual inputs as in the source initial learning, our model fixes the shared visual encoder and updates the policy decoder using the new target embodied loss.

formation which should better transfer to new tasks than arbitrary latent features. For example, the latent features from a purely end-to-end learned model may represent a variety of different (sometimes spurious) correlations, while our features must contain enough information to reconstruct depth and surface normals etc., so the network should be able to, for instance, avoid obstacles using the exact same features. While this implies that the selection of an appropriate auxiliary task affects the success of our method, if necessary our network can still be trained end-to-end using the pretrained weights as initialization.

In the specific cases of transferring from Point-Nav to Exploration or Flee we initialize the model with the weights from the **BC, PPO** setting and update the policy decoder layers using PPO with the new reward functions:

$$r_t^{explore} = \|Visited_t\| - \|Visited_{t-1}\| + \lambda_T \quad (7)$$

$$r_t^{flee} = Geo(P_t, P_{t_0}) - Geo(P_{t-1}, P_{t_0}) + \lambda_T \quad (8)$$

where $\|Visited_t\|$ represents how many unique spatial locations the agent has visited at time t .

4. Experiments

To evaluate visual navigation tasks we use the Habitat scene renderer [20] on scenes from the SUNCG [30], Matterport 3D (MP3D) [3] and Gibson [35] datasets.

4.1. Baselines

We compare our results against traditional end-to-end (E2E) training algorithm results for all experiments. These can be trained via the PPO algorithm, via behavioral cloning (BC), or pretrained with BC and finetuned with PPO. One common technique across deep learning is to pretrain models on ImageNet [5], and finetune the entire network on the desired task, which we also include as a baseline. We do

not freeze any weights when training E2E methods. We additionally include blind (but learned) agents for each task and random-action agents to benchmark task difficulty. For Point-Nav, we also include a Blind Goal Follower which aligns itself in the direction of goal vector and moves forward, realigning after it collides with obstacles.

4.2. Generalization to Unseen Environments

The ability for an algorithm to generalize to unseen environments represents its effectiveness in real-world scenarios. To begin analyzing our model, we experiment with the standard protocol of training and evaluating on data from the same simulator, partitioning the scenes into train and test. We compare performance for the Point-Nav task on three simulators (SUNCG [30], MP3D [3], Gibson [35]) evaluating in never-before-seen scenes. We use the SPL metric proposed in [1] which can be stated as

$$SPL = \frac{1}{N} \sum_{i=1}^N S_i \frac{\ell_i}{\max(p_i, \ell_i)} \quad (9)$$

where S_i is a success indicator for episode i , p_i is the path length, and ℓ_i is the shortest path length. This combines the accuracy (success) of a navigation method with its efficiency (path length) where 1.0 would be an oracle agent.

Effective policies generalize by understanding the geometry of the scenes rather than trying to localize into a known map based on the visual inputs. SplitNet outperforms all other methods by a wide margin on all three environments

	SUNCG [30]		MP3D [3]		Gibson [35]	
	SPL	Success	SPL	Success	SPL	Success
Random	0.012	0.027	0.011	0.016	0.046	0.028
Blind Goal Follower	0.199	0.203	0.155	0.158	0.325	0.319
Blind BC	0.159	0.323	0.232	0.382	0.351	0.603
Blind BC, PPO	0.291	0.377	0.317	0.471	0.427	0.643
Blind PPO	0.258	0.371	0.313	0.463	0.538	0.822
E2E PPO	0.324	0.529	0.322	0.477	0.634	0.831
E2E BC	0.343	0.548	0.459	0.737	0.509	0.824
E2E BC, PPO	0.393	0.593	0.521	0.733	0.606	0.869
ImageNet Pretrain, E2E BC	0.280	0.499	0.315	0.552	0.548	0.843
ImageNet Pretrain, E2E BC, PPO	0.338	0.440	0.450	0.539	0.642	0.737
SplitNet BC	0.421	0.687	0.517	0.808	0.584	0.865
SplitNet BC, PPO	0.560	0.703	0.716	0.844	0.701	0.855

Table 1. **Performance on Unseen Environments.** Blind methods are not provided with visual input but still receive an updated goal vector. “BC, PPO” methods are first trained with a softmax loss to take the best next action and are finetuned with the PPO algorithm.

(shown in Table 1). Surprisingly, pretraining on ImageNet does not offer better generalization, likely because the features required for ImageNet are sufficiently different from those needed to navigate effectively (note, the convolutional weights trained on ImageNet *are not frozen* during BC and PPO training). This is true even compared to E2E without pretraining on ImageNet.

As qualitative intuition about the performance of the various methods, we depict the policies for a subset of methods on an example MP3D episode from in Figure 5. For a fixed start (blue diamond) and goal (green star) location, we show the output trajectory from each method where the trajectory color (ranging from blue to red) denotes the number of steps so far. If a policy failed to reach the goal, the final destina-

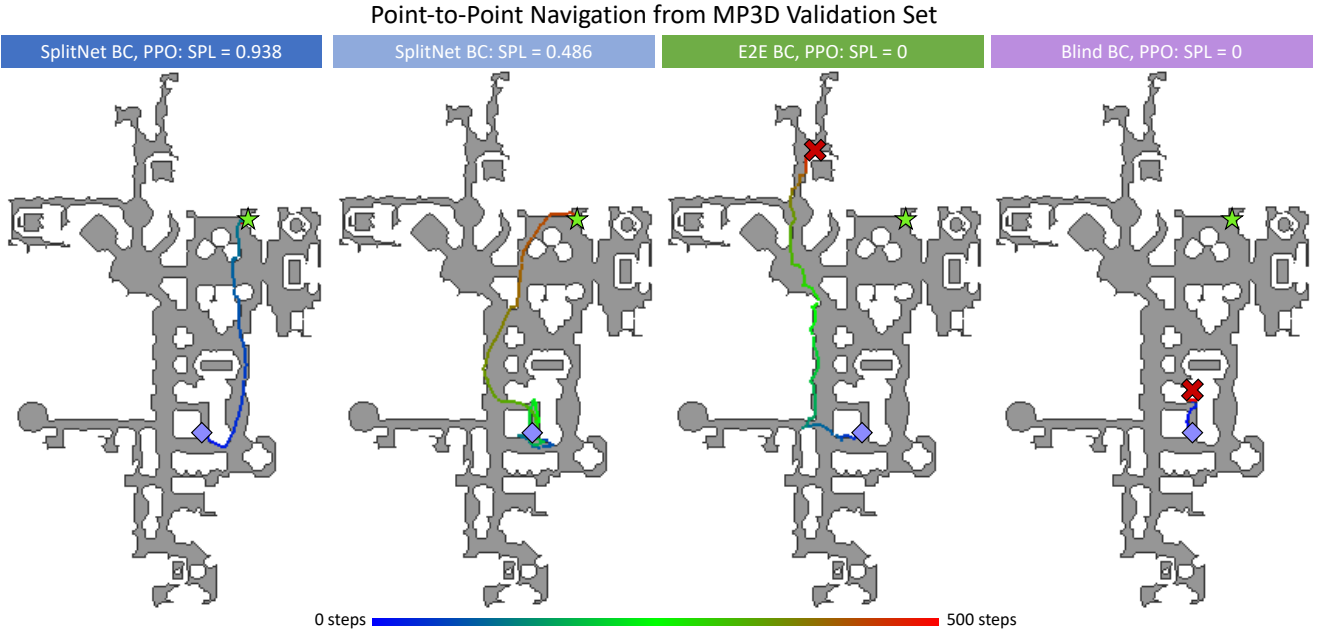


Figure 5. **Qualitative comparison of Point-Nav policies on MP3D validation.** An exemplar validation episode (fixed start and end location) and the predicted trajectories from baselines and SplitNet.

	Number Train Scenes		Test Data		Number Train Scenes		Test Data	
	SUNCG	MP3D (Train)	MP3D (Val)		MP3D	Gibson (Train)	Gibson (Val)	
	(Source)	(Target)	SPL	Success	(Source)	(Target)	SPL	Success
Source E2E BC, PPO	990	0	0.257	0.412	61	0	0.609	0.866
Source SplitNet BC, PPO	990	0	0.376	0.539	61	0	0.651	0.764
Target E2E BC	0	1	0.211	0.321	0	1	0.396	0.589
Target E2E Finetune	990	1	Failure	Failure	61	1	Failure	Failure
Target SplitNet Transfer	990	1	0.447	0.596	61	1	0.686	0.822
Target E2E BC	0	10	0.259	0.463	0	10	0.501	0.782
Target E2E Finetune	990	10	0.401	0.612	61	10	0.667	0.870
Target SplitNet Transfer	990	10	0.531	0.681	61	10	0.727	0.854
Target E2E BC, PPO	0	All (61)	0.521	0.733	0	All (72)	0.606	0.869
Target SplitNet BC, PPO	0	All (61)	0.716	0.844	0	All (72)	0.701	0.855

Table 2. **Performance transferring across simulation environments (Sim2Sim)**. Our method, SplitNet, significantly outperforms the end-to-end (E2E) baseline at the task of transferring across simulated environments. For reference, we also report the performance of a source only trained model (top two rows) or a target only trained model (bottom two rows). “Failure” indicates that performance on the target data decreases after finetuning.

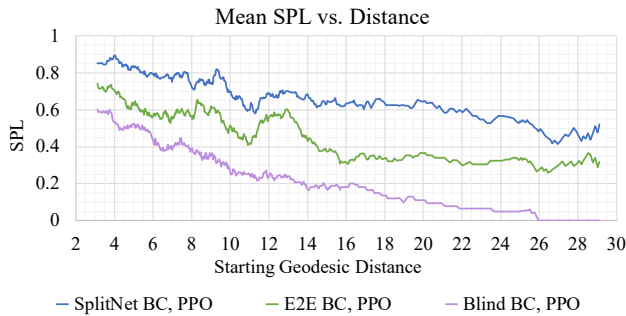


Figure 6. **MP3D Point-Nav Performance vs episode difficulty**. We compare our method, SplitNet, to end-to-end (E2E) and blind learned baselines and report SPL performance as a function of starting geodesic distance from the goal. SplitNet outperforms on all starting distances, especially on the more difficult episodes.

tion is denoted with a red “x”. From this visualization we can see that SplitNet using BC and PPO successfully completes the task and does so with the shortest overall path. At the beginning of the episode SplitNet BC is stuck behind the wall, but eventually is able to navigate away from the wall and reach the target.

We further analyze the performance of SplitNet compared to baselines as a function of the geodesic distance between the starting and goal locations in Figure 6. This distance is highly correlated with the difficulty of an episode. Unsurprisingly, all methods degrade as the starting location is moved further from the goal location, but SplitNet retains its advantage over baselines irrespective of the episode difficulty. Additionally, we see the performance gap widen over the more difficult episodes, meaning we handle difficult episodes better than the baselines.

4.3. Transfer Across Simulators

We now study the ability for our method to transfer between visual environments for the fixed task of Point-Nav. We denote *Source* to be the initial simulator in which we train our model using both BC and PPO and denote this initial model as “Source SplitNet BC, PPO.” The baseline source model that uses end-to-end training is denoted as “Source E2E BC, PPO.” We then compare our method for transfer to the new simulator *Target*, described in Section 3.5.1 and denoted as “Target SplitNet Transfer,” against the end-to-end baseline finetuned on the target, “Target E2E Finetune.” For reference, we also present the performance of training an end-to-end model using only the available target data, denoted as “Target E2E BC.”

Table 2 reports our main results for this Sim2Sim transfer problem as a function of the amount of available target scenes during training. We report performance for the two transfer settings of SUNCG→MP3D and MP3D→Gibson. These simulators differ in terms of complexities of differing rendering appearance (as seen in Figure 1), different environment construction methods (synthetic vs. depth-scan reconstruction), and different environment size. Again, SplitNet outperforms all baselines across all experiments in terms of the SPL metric and performs better or comparable to the baseline in terms of success for all transfer setups. Even with no extra data, our initially learned network is more generalizable to new environments, especially those which are significantly different in appearance (SUNCG→MP3D). Of note, in both cases, SplitNet given 10 scenes from the target dataset matches or outperforms the end-to-end baseline SPL given the entire target dataset.

Note, that our approach to visual environment transfer

SplitNet Model	Layers Finetuned	Number Target Scenes	SPL	Success
<i>Transfer SUNCG → MP3D (train): Eval MP3D (val)</i>				
Source Only	-	-	0.376	0.539
Finetune Target	V+P	1	0.435	0.586
Finetune Target	V	1	0.447	0.596
Finetune Target	V+P	10	0.400	0.552
Finetune Target	V	10	0.531	0.681
<i>Transfer MP3D → Gibson (train): Eval Gibson (val)</i>				
Source Only	-	-	0.651	0.764
Finetune Target	V+P	1	Failure	Failure
Finetune Target	V	1	0.686	0.822
Finetune Target	V+P	10	Failure	Failure
Finetune Target	V	10	0.727	0.854

Table 3. **Ablation of SplitNet Sim2Sim transfer strategy.** SplitNet only updates the visual encoder (“V”) and fixes the policy decoder (“P”) when finetuning the source SplitNet model on a target visual environment. In contrast, finetuning both V+P on the target leads to degraded performance.

includes finetuning only the visual encoder in the target environment and leaving the policy decoder fixed. One may wonder whether this is the optimal approach or whether our method would benefit from target updates to the policy decoder as well. To answer this question, in Table 3 we report performance comparing the initial source SplitNet performance to that of finetuning either only the visual encoder (“V”) which is our proposed approach or finetuning both the visual encoder and policy decoder (“V+P”). Interestingly, we found that allowing updates to both the visual encoder and policy decoder in the target environment lead to significant overfitting which resulted in failed generalization to the unseen scenes from the validation sets. This confirms the benefit of our split training approach.

4.4. Transfer Across Tasks

We test the ability for SplitNet to learn a new task by first training the network on Point-Nav and using our approach to transfer the model to the novel tasks of Exploration and Flee. All three tasks require the ability to transform 2D visual inputs into 3D scene geometry, but the decisions about what to do based on the perceived geometry are drastically different. Since SplitNet decouples the policy from the perception, it learns features which readily transfer to a novel, but related task.

Figure 7 shows that SplitNet immediately begins to learn effective new policies, outperforming the other methods almost right away. In Exploration, our method is able to reuse its understanding of depth to quickly learn to approach walls, then turn at the last second and head off in a new direction. For the Flee task, our method identifies long empty hallways and navigates down those away from the start location. None of the other methods learn

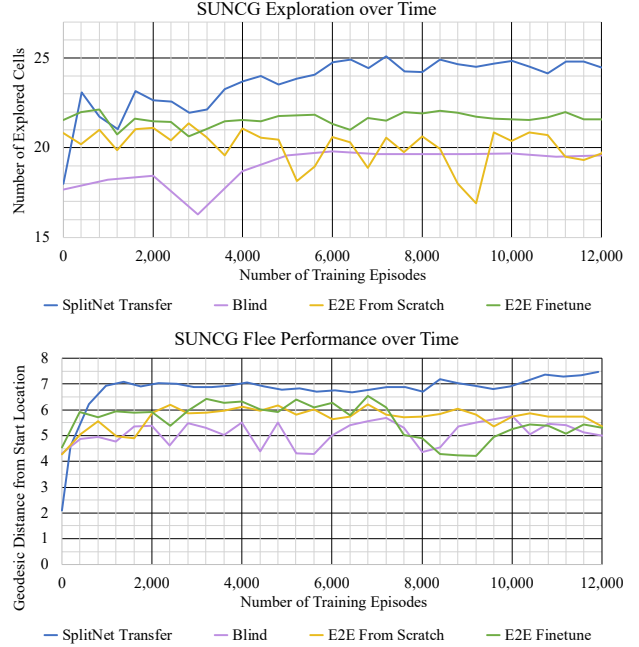


Figure 7. **SUNCG Task2Task performance as a function of target training episodes.** SplitNet Transfer and E2E Transfer are first trained on SUNCG Point-Nav, but SplitNet only updates the policy layers whereas E2E updates the entire network. E2E from scratch is randomly initialized a episode 0. The Blind method only receives its previous action as input and is randomly initialized.

robust obstacle-avoidance behavior or geometric scene understanding, which can be seen in our supplemental video. Instead they latch on to simple dataset biases such as “repeatedly move forward then rotate.”

4.5. Analysis of Auxiliary Objectives

Our method was designed as a solution for generalization on a downstream embodied task. However, SplitNet also learns outputs for the auxiliary visual and motion tasks. While our goal is not to surpass state-of-the-art performance on these auxiliary tasks it is still useful to verify that the visual encodings match our expectations. We therefore created videos which show both intermediate outputs, actions taken, and an overall predicted trajectory for SplitNet and baseline methods. As this result is best viewed in the video format, we refer the interested reader to the supplementary material to view this result. We show excerpts where the encoder and decoders from SplitNet are able to perform both the visual and motion based auxiliary tasks leading us to conclude that the expected geometric information is present within the representation from the visual encoder.

5. Conclusion

We introduce SplitNet, a method for decomposing embodied learning tasks to enable fast and accurate transfer to new environments and new tasks. By disentangling the

visual encoding of the state from the policy for a task, we learn more robust features which can be frozen or adapted based on the changed domain. Our model matches the performance of end-to-end methods even with six times less data. We believe SplitNet may prove to be a useful stepping stone in transferring networks from simulation environments onto robots in the real-world.

References

- [1] P. Anderson, A. Chang, D. S. Chaplot, A. Dosovitskiy, S. Gupta, V. Koltun, J. Kosecka, J. Malik, R. Mottaghi, M. Savva, et al. On evaluation of embodied navigation agents. *arXiv preprint arXiv:1807.06757*, 2018. **6**
- [2] K. Bousmalis, N. Silberman, D. Dohan, D. Erhan, and D. Krishnan. Unsupervised pixel-level domain adaptation with generative adversarial networks. In *Computer Vision and Pattern Recognition (CVPR)*, 2017. **2**
- [3] A. Chang, A. Dai, T. Funkhouser, M. Halber, M. Niessner, M. Savva, S. Song, A. Zeng, and Y. Zhang. Matterport3D: Learning from RGB-D data in indoor environments. In *International Conference on 3D Vision (3DV)*, 2017. **1, 5, 6**
- [4] K. Cho, B. van Merriënboer, C. Gulcehre, D. Bahdanau, F. Bougares, H. Schwenk, and Y. Bengio. Learning phrase representations using rnn encoder–decoder for statistical machine translation. In *Proceedings of the 2014 Conference on Empirical Methods in Natural Language Processing (EMNLP)*, pages 1724–1734, 2014. **4**
- [5] J. Deng, W. Dong, R. Socher, L.-J. Li, K. Li, and L. Fei-Fei. ImageNet: A Large-Scale Hierarchical Image Database. In *Computer Vision and Pattern Recognition (CVPR)*, 2009. **2, 5**
- [6] Y. Ganin and V. Lempitsky. Unsupervised domain adaptation by backpropagation. In D. Blei and F. Bach, editors, *Proceedings of the 32nd International Conference on Machine Learning (ICML-15)*, pages 1180–1189. JMLR Workshop and Conference Proceedings, 2015. **2**
- [7] R. Girshick, J. Donahue, T. Darrell, and J. Malik. Rich feature hierarchies for accurate object detection and semantic segmentation. In *Computer Vision and Pattern Recognition (CVPR)*, 2014. **2, 5**
- [8] Y. Goyal, T. Khot, D. Summers-Stay, D. Batra, and D. Parikh. Making the V in VQA matter: Elevating the role of image understanding in Visual Question Answering. In *Computer Vision and Pattern Recognition (CVPR)*, 2017. **5**
- [9] S. Gupta, J. Davidson, S. Levine, R. Sukthankar, and J. Malik. Cognitive mapping and planning for visual navigation. In *Computer Vision and Pattern Recognition (CVPR)*, pages 2616–2625, 2017. **2**
- [10] J. Hoffman, E. Tzeng, T. Park, J.-Y. Zhu, P. Isola, K. Saenko, A. A. Efros, and T. Darrell. Cycada: Cycle-consistent adversarial domain adaptation. In *International Conference in Machine Learning (ICML)*, 2018. **2**
- [11] J. Hoffman, D. Wang, F. Yu, and T. Darrell. Fcns in the wild: Pixel-level adversarial and constraint-based adaptation. *CoRR*, abs/1612.02649, 2016. **2**
- [12] H. Huang¹, Q. Huang², and P. Krahenbuhl. Domain transfer through deep activation matching. In *European Conference on Computer Vision (ECCV)*, 2018. **2**
- [13] J. Long*, E. Shelhamer, and T. Darrell. Fully convolutional networks for semantic segmentation. In *Computer Vision and Pattern Recognition (CVPR)*, 2015. **5**
- [14] M. Jaderberg, V. Mnih, W. M. Czarnecki, T. Schaul, J. Z. Leibo, D. Silver, and K. Kavukcuoglu. Reinforcement learning with unsupervised auxiliary tasks. In *International Conference in Learning Representations (ICLR)*, 2017. **2**
- [15] E. Kolve, R. Mottaghi, W. Han, E. VanderBilt, L. Weihs, A. Herrasti, D. Gordon, Y. Zhu, A. Gupta, and A. Farhadi. AI2-THOR: An Interactive 3D Environment for Visual AI. *arXiv*, 2017. **1**
- [16] S. Levine, C. Finn, and T. D. and Pieter Abbeel. End-to-end training of deep visuomotor policies. *Journal of Machine Learning Research (JMLR)*, 2016. **2**
- [17] S. Levine, P. Pastor, A. Krizhevsky, J. Ibarz, and D. Quillen. Learning hand-eye coordination for robotic grasping with deep learning and large-scale data collection. *The International Journal of Robotics Research*, 37(4-5):421–436, 2018. **2**
- [18] M.-Y. Liu and O. Tuzel. Coupled generative adversarial networks. In *Neural Information Processing Symposium (NeurIPS)*, 2016. **2**
- [19] M. Long, Y. Cao, J. Wang, and M. I. Jordan. Learning transferable features with deep adaptation networks. In *International Conference in Machine Learning (ICML)*, 2015. **2**
- [20] M. Savva*, A. Kadian*, O. Maksymets*, Y. Zhao, E. Wijmans, B. Jain, J. Straub, J. Liu, V. Koltun, J. Malik, D. Parikh, and D. Batra. Habitat: A platform for embodied ai research. *arXiv preprint arXiv:1904.01201*, 2019. **1, 5**
- [21] P. Mirowski, R. Pascanu, F. Viola, H. Soyer, A. J. Ballard, A. Banino, M. Denil, R. Goroshin, L. Sifre, K. Kavukcuoglu, D. Kumaran, and R. Hadsell. Learning to navigate in complex environments. In *International Conference in Learning Representations (ICLR)*, 2017. **2**
- [22] V. Mnih, A. P. Badia, M. Mirza, A. Graves, T. Lillicrap, T. Harley, D. Silver, and K. Kavukcuoglu. Asynchronous methods for deep reinforcement learning. In *International conference on machine learning*, pages 1928–1937, 2016. **2**
- [23] M. Müller, A. Dosovitskiy, B. Ghanem, and V. Koltun. Driving policy transfer via modularity and abstraction. In *European Conference on Computer Vision (ECCV)*, 2018. **3**
- [24] D. Pathak, P. Agrawal, A. A. Efros, and T. Darrell. Curiosity-driven exploration by self-supervised prediction. In *Proceedings of the IEEE Conference on Computer Vision and Pattern Recognition Workshops*, pages 16–17, 2017. **2**
- [25] X. B. Peng, M. Andrychowicz, W. Zaremba, and P. Abbeel. Sim-to-real transfer of robotic control with dynamics randomization. In *2018 IEEE International Conference on Robotics and Automation (ICRA)*, pages 1–8. IEEE, 2018. **1, 3**
- [26] A. Radford, L. Metz, and S. Chintala. Unsupervised representation learning with deep convolutional generative adversarial networks. In *International Conference in Learning Representations (ICLR)*, 2016. **2**

- [27] A. A. Rusu, M. Večerík, T. Rothörl, N. Heess, R. Pascanu, and R. Hadsell. Sim-to-real robot learning from pixels with progressive nets. In *Conference on Robot Learning (CoRL)*, pages 262–270, 2017. 1, 2
- [28] A. Sax, B. Emi, A. R. Zamir, L. J. Guibas, S. Savarese, and J. Malik. Mid-level visual representations improve generalization and sample efficiency for learning active tasks. *CoRR*, abs/1812.11971, 2018. 2
- [29] J. Schulman, F. Wolski, P. Dhariwal, A. Radford, and O. Klimov. Proximal policy optimization algorithms. *arXiv preprint arXiv:1707.06347*, 2017. 4
- [30] S. Song, F. Yu, A. Zeng, A. X. Chang, M. Savva, and T. Funkhouser. Semantic scene completion from a single depth image. In *Computer Vision and Pattern Recognition (CVPR)*, 2017. 5, 6
- [31] B. Sun and K. Saenko. Deep coral: Correlation alignment for deep domain adaptation. In *European Conference on Computer Vision (ECCV)*, 2016. 2
- [32] Y. Taigman, A. Polyak, and L. Wolf. Unsupervised cross-domain image generation. In *International Conference in Learning Representations (ICLR)*, 2017. 2
- [33] J. Tobin, R. Fong, A. Ray, J. Schneider, W. Zaremba, and P. Abbeel. Domain randomization for transferring deep neural networks from simulation to the real world. In *2017 IEEE/RSJ International Conference on Intelligent Robots and Systems (IROS)*, pages 23–30. IEEE, 2017. 1, 2, 3
- [34] E. Tzeng, J. Hoffman, T. Darrell, and K. Saenko. Adversarial discriminative domain adaptation. In *Computer Vision and Pattern Recognition (CVPR)*, 2017. 2
- [35] F. Xia, A. R. Zamir, Z. He, A. Sax, J. Malik, and S. Savarese. Gibson env: Real-world perception for embodied agents. In *Computer Vision and Pattern Recognition (CVPR)*, 2018. 1, 5, 6
- [36] C. Yan, D. Misra, A. Bennnett, A. Walsman, Y. Bisk, and Y. Artzi. CHALET: Cornell house agent learning environment. *arXiv:1801.07357*, 2018. 1
- [37] A. R. Zamir, A. Sax, W. B. Shen, L. J. Guibas, J. Malik, and S. Savarese. Taskonomy: Disentangling task transfer learning. In *Computer Vision and Pattern Recognition (CVPR)*. IEEE, 2018. 2
- [38] J. Zhang, J. T. Springenberg, J. Boedecker, and W. Burgard. Deep reinforcement learning with successor features for navigation across similar environments. In *International Conference on Intelligent Robotics and Systems*, 2017. 2
- [39] Y. Zhang, P. David, and B. Gong. Curriculum domain adaptation for semantic segmentation of urban scenes. In *International Conference on Computer Vision (ICCV)*, 2017. 2
- [40] J.-Y. Zhu, T. Park, P. Isola, and A. A. Efros. Unpaired image-to-image translation using cycle-consistent adversarial networks. In *International Conference on Computer Vision (ICCV)*, 2017. 2
- [41] Y. Zhu, D. Gordon, E. Kolve, D. Fox, L. Fei-Fei, A. Gupta, R. Mottaghi, and A. Farhadi. Visual semantic planning using deep successor representations. In *International Conference on Computer Vision (ICCV)*, pages 483–492, 2017. 2
- [42] Y. Zhu, R. Mottaghi, E. Kolve, J. J. Lim, A. Gupta, L. Fei-Fei, , and A. Farhadi. Target-driven visual navigation in indoor scenes using deep reinforcement learning. In *International Conference on Robotics and Automation (ICRA)*, 2017. 2

Dataset	Number of Train Scenes	Number of Train Episodes	Number of Val Scenes	Number of Val Episodes
SUNCG	990	898267	905	99
MP3D	61	5000000	495	11
Gibson	72	4932479	1000	16

Table A1. Dataset Statistics

Appendix A. Video

In our attached video we show example trials of SplitNet as well as several baselines. The video includes:

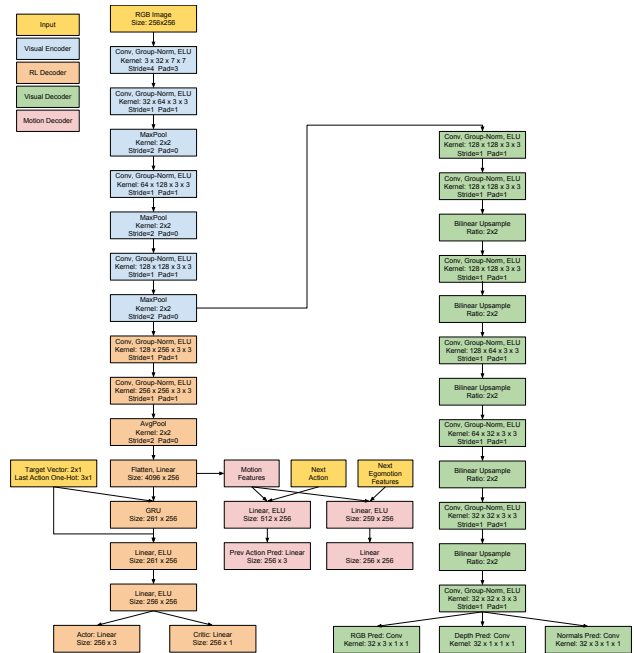
1. SplitNet examples showing the auxiliary visual tasks from SUNCG and MP3D.
2. Sim2Sim transfer (SUNCG \rightarrow MP3D) examples showing SplitNet using 0, 1, 10, and all target scenes for training.
3. Sim2Sim transfer (SUNCG \rightarrow MP3D) examples showing E2E using 0, 1, 10, and all target scenes for training.
4. Task2Task transfer (Point-Nav \rightarrow Exploration and Flee) of SplitNet and E2E as well as E2E From Scratch and Blind agents.
5. Point-Nav examples on Gibson, MP3D, and SUNCG for SplitNet, E2E, and Blind agents.

Appendix B. Dataset Details

We constructed the Point-Nav datasets for each of SUNCG, MP3D, and Gibson environments using a sampling-based method which filtered out easy episodes (those with $\frac{\text{euclidean distance}}{\text{geodesic distance}} < 1.1$). We additionally filter out episodes where there is no path between the start and goal location. The start points from these episodes were additionally used for the Exploration and Flee tasks, but the goal locations were ignored. Per-environment statistics are listed in Table A1.

Appendix C. Network Architecture

Figure F1 shows the encoder-decoder architecture of SplitNet. The E2E method trains the blue and orange portions, and the blind agent trains only the orange. Additionally the Motion layers are only trained for SplitNet. Those are omitted for simplicity due to them operating on multiple timesteps. The Egomotion

Figure F1. **SplitNet Architecture**